AAPS PharmSciTech 2002; 3 (4) article 29 (http://www.aapspharmsci.org).

Crystal Doping Aided by Rapid Expansion of Supercritical Solutions

Submitted: July 18, 2002; Accepted: September 20, 2002

Chandra Vemavarapu [1,2], Matthew J. Mollan [1] and Thomas E. Needham [2]

[1]Pharmaceutical Sciences, Pfizer Global R&D, Ann Arbor, MI 48105

[2]Applied Pharmaceutical Sciences, University of Rhode Island, Kingston, RI 02881

ABSTRACT The purpose of this study was to test the utility of rapid expansion of supercritical solution (RESS) based cocrystallizations in inducing polymorph conversion and crystal disruption of chlorpropamide (CPD). CPD crystals were recrystallized by the RESS process utilizing supercritical carbon dioxide as the solvent. The supercritical region investigated for solute extraction ranged from 45 to 100°C and 2000 to 8000 psi. While pure solute recrystallization formed stage I of these studies, stage II involved recrystallization of CPD in the presence of urea (model impurity). The composition, morphology, and crystallinity of the particles thus produced were characterized utilizing techniques such as microscopy, thermal analysis, x-ray powder diffractometry, and high-performance liquid chromatography. Also, comparative evaluation between RESS and evaporative crystallization from liquid solvents was performed. RESS recrystallizations of commercially available CPD (form A) resulted in polymorph conversion to metastable forms C and V, depending on the temperature and pressure of the recrystallizing solvent. Cocrystallization studies revealed the formation of eutectic mixtures and solid solutions of CPD + urea. Formation of the solid solutions resulted in the crystal disruption of CPD and subsequent amorphous conversion at urea levels higher than 40% wt/wt. Consistent with these results were the reductions in melting point (up to 9°C) and in the ΔH_f values of CPD (up to 50%). Scanning electron microscopy revealed a particle size reduction of up to an order of magnitude upon RESS processing. Unlike RESS, recrystallizations from liquid organic solvents lacked the ability to affect polymorphic conversions. Also, the incorporation of urea into the lattice of CPD was found to be inadequate. In providing the ability to control both the particle and crystal morphologies of active pharmaceutical ingredients, RESS proved potentially advantageous to crystal engineering. Rapid crystallization kinetics were found vital in making RESS-based doping superior to conventional solvent-based cocrystallizations.

Correspondence to:
Chandra Vemavarapu,
Pharmaceutical Sciences
Pfizer Global R&D
Ann Arbor, MI 48105
Telephone: (734) 622-4823
Facsimile: (734) 622-7799
E-mail: chandra.vemavarapu@pfizer.com

KEYWORDS: Rapid expansion of supercritical solutions, RESS, crystal doping, cocrystallization, chlorpropamide, urea

INTRODUCTION The role of residual impurities on the bulk physical properties of a crystalline substance has long been identified and is generally regarded to be adverse. The residual impurities often include unused reactants, catalysts, synthetic byproducts, chiral isomers, solvates, hydrates, surfactants, monomers, and so forth that develop during synthesis, extraction, recrystallization, and storage. Although often challenging, the cleanup task is achieved by secondary recrystallization methods or by alternative methods of synthesis. In instances where purification beyond a certain level is not practical, the effects of the presence of impurities on the efficacy, safety, and stability profiles of the active pharmaceutical ingredient (API) have been established. Such studies have revealed a domain of effects that an impurity can have on the crystal morphology and crystal energetics of an API. While this awareness of the role of impurities manifested as an additional burden to the traditional synthetic chemist, it also opened up a realm of new science called supramolecular chemistry. Broadly defined as the science that deals with anything outside the scope of covalent chemistry, supramolecular chemistry involves selective incorporation of tailor-made additives and impurities into the crystal lattice of a host substance. Incorporation of the additives is based on interactions such as H-bonding, ion pairing, van der Waals attractive forces, hydrophobic interactions, beta-stacking, and nonspecific inclusion [1-3].Design of composite materials with altered bulk properties is made possible through such crystal modification. Supramolecular chemistry combines the features of contemporary stereochemistry and biological enzyme-ligand

Table 1. Nomenclature/Properties of Reported Chlorpropamide Polymorphs*

Polymorph	Source	T_m (°C)	ΔH_f (J/g)	ΔH_f [16] (J/g)	Characteristic XRPD Peak (2θ)	Habit
A[15]/ III[13]/IV[14]	Commercial	121-122	100.22	21.25	6.62, 11.78	Tabular
B[15]/II[13]/V[14]	Recrystallization from melt	124-127	77.03	15.22	12.36	Blades
C[15]/I[13,14]	Heat A @120°C for 3 hrs	128-130	85.77	36.07	15.18	Plates
IV[13]	Crystallization from CCl_4	122-123	NR	NR	NR	NR
V[13]	Desolvation of solvate of benzene	<118	NR	NR	NR	NR
II[14]	Rapid evaporation from chloroform	NR	NR	NR	NR	NR
III[14]	Rapid cooling from hexanol	NR	NR	NR	NR	NR

*XRPD indicates x-ray powder diffractometry; NR, not reported.

systems in engineering crystal morphologies. Crystal engineering based on this science afforded among other applications a considerable promise in habit modification [4], racemate isolation [5], doping-mediated induction of crystal defects [6], and amorphous conversion, preferential crystallization of the favored polymorph [7-8], and synthesis of new molecular complexes [9].

A theoretical basis for the role of additives at molecular and bulk levels that will allow precise control over tailoring crystals still remains to be established. Efforts at such an understanding have mostly been limited to inorganics and other small molecules. The complexity of multiple conformations while dealing with pharmaceutically relevant molecules makes extension of such theories to pharmaceuticals rather difficult and may be the cause of limited progress in this area. While the advancement of supramolecular chemistry in disciplines such as ceramics, photography, and semiconductors has therefore been significant, the concept is still at its inception in pharmaceuticals and has only occasionally been reported [8,10-12].This body of work is intended to serve as a proof of concept for the application of supramolecular chemistry in drug development. In particular, this work is designed to evaluate crystal doping by recrystallization from supercritical media. The rapid nucleation and growth implicit in supercritical fluid (SCF) based crystallizations provided the motivation for choosing the rapid expansion of supercritical solution (RESS) process. The ultimate motive in producing doped crystals is to add functionality to APIs at early stages of chemical synthesis. For example, producing low-energy forms of the crystals can enhance the dissolution rates of poorly soluble drugs. Alternatively, crystallization of the most favored polymorph can be induced through doping. Such studies can prove particularly viable and timely in the context of the recent emphasis on the integration of the discovery and development research in pharmaceutical industry. For the purposes of this study, chlorpropamide (CPD) was chosen as a model API and urea as the model dopant. The rationale for the selection of this API-dopant mixture was based on the structural similarity between the API and the dopant. In addition, doping is more controllable with a small molecule such as urea and in theory will reduce the propensity for segregation and associated stability problems.

CPD belongs to the sufonyl urea class of oral hypoglycemics. It is known to be practically insoluble in water and belongs to class II of biopharmaceutical classification. Five different polymorphs of CPD have been identified to date, of which 3 are most commonly referred to in the published literature [13-16].As is often the case with APIs exhibiting multiple conformations, a standardized nomenclature does not exist for the various forms of CPD (**Table 1**). For the purposes of consistency, the notation defined by Simmons et al [15].is followed in this study. Even after the 3 decades since it was discovered, it is interesting to note that polymorphism in CPD has not been completely characterized. The specific objectives of this study are therefore to characterize the various polymorphs of CPD prior to evaluating the efficacy of the RESS process in doping CPD with urea.

MATERIALS AND METHODS

Materials

The CPD used in these studies was bought from Sigma (St Louis, MO, Lot 31H0722), and the urea from JT Baker (Phillipsburg, NJ, Lot N37340). All the solvents used were from JT Baker and are of high-performance liquid chromatography (HPLC) grade.

Methods

Crystallization From Supercritical Solvent

The RESS process was used in the cocrystallization of solid active pharmaceuticals and their structurally related impurities. In this process, the solutes of interest were dissolved in SC CO_2, forming a homogeneous supercritical solution. Nucleation of solutes was then induced by rapidly reducing the solution density through expansion to atmospheric conditions. A rapid decrease in solvent strength results in high supersaturation that leads to very high homogeneous nucleation rates [17].The time for nucleation and growth is very limited (typically $10^{-5}$to 10^{-6}seconds), resulting in very small particles [18-19].Although catastrophic in nature, homogeneous nu

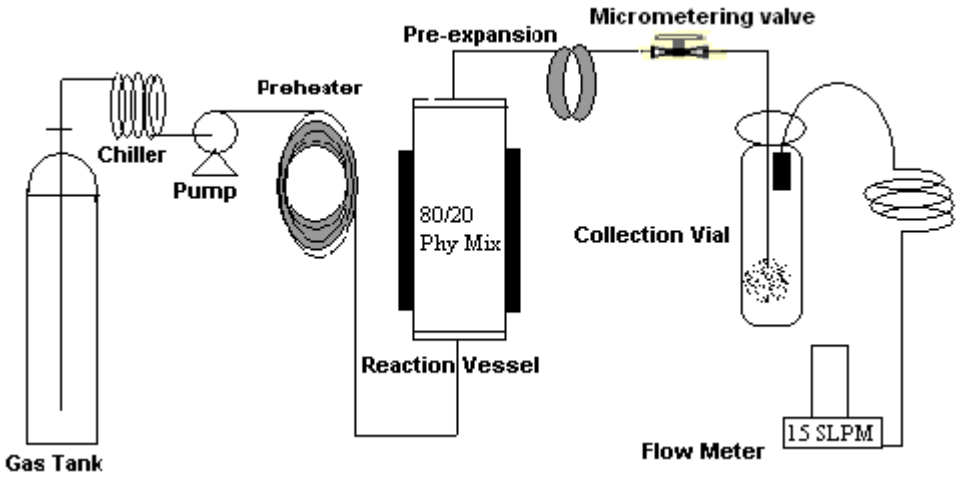

Figure 1. Schematic of RESS process for crystal doping. SLPM indicates standard liters per minute.

cleation in the RESS process is much more controllable compared to the nucleation from liquids, because of RESS's ability to easily control the supersaturation ratio. Also, the rapid nucleation and growth aids in locking the impurities into the crystal domains of the hosts by not providing sufficient time for the impurities to segregate. Absence of residual liquid solvents in the RESS-produced crystals further reduces the possibility for segregation in the solid state.

In addition, the rapid decompression of SCF generates mechanical perturbation within the solution that travels at the speed of sound [18].Consequently, very uniform conditions are reached within the nucleating media. Uniform conditions in the nucleating media assist in homogeneous dispersion of impurities in the crystal domains of the hosts. The crystal disruption following such uniform and rapid cocrystallization can be expected to be controlled and large [20].All the above factors contributed to the special interest in RESS-aided crystal doping and formed the rationale for its choice.

Commercially available SCF extraction equipment (SFT150, Supercritical Fluid Technologies Inc, Newark, DE) was reconfigured to produce cocrystals of drugs and impurities by the RESS process (**Figure 1**). Liquid CO_2 from a tank was pressurized using an air-driven Haskel pump and fed to the preheater. The preheater served as a heat exchanger in raising the temperature of the pressurized liquid to the supercritical region. The preheater used was a 5-meter stainless steel coil wrapped with rope heaters (FGR, Omega Engineering Inc, Stamford, CT). The temperature of the preheater was controlled within ±1°C using a temperature controller (Glas-Col, Terre Haute, IN). Supercritical $CO_2$from the preheater was then fed to the 100-mL reaction vessel that contained the solutes to be recrystallized. The temperature of the reaction vessel's contents was controlled to within ±1.5°C using external band heaters and internally placed resistive temperature devices (RTD), both in communication with a PID temperature controller. All the pressure values reported in this manuscript were read using a bourdon tube gauge with an accuracy of ±100 psi and should be treated as gauge pressures. The reproducibility of the experiments following the above controls was found to be adequate (<5% RSD) for the purposes of this study.

The reaction vessel was typically packed with 90 g of 3-mm glass beads and 10 g of solutes. The glass beads assist in improving the efficiency of extraction while also buffering the turbulent flow of the fluid through the vessel. The starting mixture in the reaction vessel consisted of a physical blend of 80% drug and 20% impurity. Placing glass wool at both ends of the reaction vessel supported the powder bed and also prevented the entrainment of solutes. Depending on the selectivity of extraction of the supercritical solvent, saturated solutions form in the reaction vessel with fixed compositions of the host and impurity. The saturated SCF solution from the reaction vessel flowed through a 0.5-µm stainless steel frit into the preexpansion chamber. The preexpansion chamber was maintained at 50°C above the extraction temperature. Cold spots and abrupt temperature drops in the lines were found to cause premature precipitation of solutes, which in turn led to plugging of lines. All the lines and connectors therefore were heated using Omega rope heaters controlled by a Glas-Col temperature controller.

The saturated solution from the preexpansion chamber then passed through a heated restriction device (micrometering valve) maintained at 100 to 150°C prior to rapid expansion. Heating the micrometering valve compensated for the Joule-Thompson cooling that occurs as a result of rapid expansion. The expansion device used was a stainless steel capillary of aspect ratio 100 (5" Length / 0.05" Internal Diameter) that was securely inserted through the snap cap of a 40-mL glass vial (Daigger, Lincolnshire, IL). Given that the interest here is in

the crystal morphology of the pharmaceutical actives rather than their particle size, a 40-mL particle collection vial was best suited for these purposes. CO_2gas after deposition of the solids was exhausted through a custom filter and passed through lengthy tubing (5 meters) prior to feeding to the thermo mass flow meter (Porter Instruments, Hatfield, PA). The gas flow rates were further totalized (Infinity Rate Totalizer, Newport Electronics, Santa Ana, CA) over the course of the experiment to get a more reliable estimate of the average CO_2 flow rates though the system. Typical flow rates of CO_2through the system were between 5 and 10 standard liters per minute (SLPM). At the end of each run, yields of the recrystallized materials were recorded and the vials were stored in low-humidity plastic bags at ambient temperature until further use.

Following the above method, CPD + urea mixtures were recrystallized and the efficiency of SCF-aided crystal doping was evaluated. The supercritical region investigated in these studies included a temperature regime of 45 to 100°C and pressures between 2000 and 8000 psi. The yields of cocrystals extracted at a pressure less than 4000 psi were too low to perform further characterization work and hence are not reported in this manuscript.

Crystallization From Liquid Organic Solvents

The role of the rapid crystallization kinetics in the SCF-aided crystal doping can be best evaluated by comparing the doped crystals from the RESS process to the ones crystallized at a much slower rate–for example, by evaporative crystallization. Toward this objective, evaporative crystallization of CPD in the presence of varying amounts of urea as the impurity was undertaken. Other solvent-related effects were in part normalized by choosing hexane (δ = 7.24 Hildebrand units) and ethyl acetate (d = 9.10 Hildebrand units) as recrystallizing solvents, which are reported to closely resemble supercritical CO_2in their solubility behavior [21-23].In addition, recrystallization from a relatively polar ethyl alcohol solvent (δ = 12.9 Hildebrand units) was also performed in order to investigate the effect of the solvent polarity on the crystal doping of CPD + urea.

Evaporative crystallization experiments were carried out using a nitrogen analytical evaporator (Myer N-Evap, Organomation Associates Inc, Berlin, MA). One gram of CPD/urea mixtures in varying proportions (100/0, 80/20, 90/10, 99/1, 99.5/0.5, and 99.9/0.1, % wt/wt basis) were accurately weighed into 40-mL glass vials. Ten milliliters of warm recrystallizing solvents at 45°C was added to these vials, and the solutions were thoroughly shaken prior to placing them in the 45°C temperature bath. Needles connected to a common nitrogen source were inserted into the head space of the vials and fixed at standard heights such that uniform conditions prevailed in the different vials. While solvent evaporation was complete in the case of hexane and ethyl acetate within 12 hours, removal of ethyl alcohol took up to 24 hours owing to the lower vapor pressure of the hydroalcoholic solution. At the end of the experiment, the recrystallized materials were spread into individual petri dishes, oven-dried at 45°C overnight, and sieved through a #60 (250 μ) screen. The screened materials were subsequently filled into vials, tightly capped and stored in low-humidity plastic bags at ambient temperature until needed for further use.

Differential Scanning Calorimetry

Accurately weighed milligram samples were scanned in pinholed aluminum pans under dry nitrogen purge. Various heating rates of 1, 2, 3, 5, and 10°C/min were used to perform differential scanning calorimetry (DSC) analysis (DSC-7, Perkin-Elmer, Norwalk, CT).

Modulated DSC

Modulated DSC (mDSC) analysis (MDSC 2920, TA Instruments, New Castle, DE) was used in an attempt to distinguish the kinetic events from the thermodynamic events in the thermal analysis of CPD. About 10 mg sampleswere accurately weighed and thermally scanned between 25 and 140°C in the pinholed, crimped aluminum pans. The scanning conditions included a heating ramp of 1°C/min with the modulation amplitude of 1°C in a 60-second period.

Hot Stage Microscopy

Thermomicroscopy of these samples was performed using a Mettler FP82-HT hot stage attached to the Mettler FP80-HT controller and a video system. (Mettler-Toledo, Inc., Columbus, OH). Changes in the particle and crystal morphologies that occurred during the heating and cooling cycles were observed using a polarized optical microscope (Wild Leitz, Heerbrugg, Switzerland).

Thermogravimetric Analysis

Thermal decomposition, moisture, and residual solvent contents of the recrystallized materials were investigated by thermogravimetric analysis (TGA-7, Perkin-Elmer, Norwalk, CT). Samples were heated at 5°C/min in an open platinum pan with the nitrogen purge at 60 mL/min.

X-ray Powder Diffractometry

X-ray powder diffractometry (XRPD) was performed using a KD-2660-N x-ray diffractometer controlled by the D-Max B controller and Datascan MDI software (Rigaku USA, Danvers, MA). The operating conditions included λ = 1.54°A, 2θ = 3° to 50°, scan speed 3°/minute, sampling interval 0.020°, and x-ray power (tube input) of 40 kV/40 mA. The path of x-rays was controlled utilizing standard slits such as 1/2° divergence, 1/2° scatter slits, 0.3-mm receiving slit, and 0.6-mm receiving monochromator slit, in that order. Depending on amounts of the samples available for XRPD analysis, the powders were either packed into the 0.2-mm groove of a glass slide (regular method) or sprinkled onto a thin film of Apiezon grease applied onto the glass slide (grease method).

Polarizing Optical Microscopy

Bulk particle morphology and the crystalline birefringence behavior of the samples were investigated using a polarizing optical microscope (Leitz Lab 12 Pol S, Wild

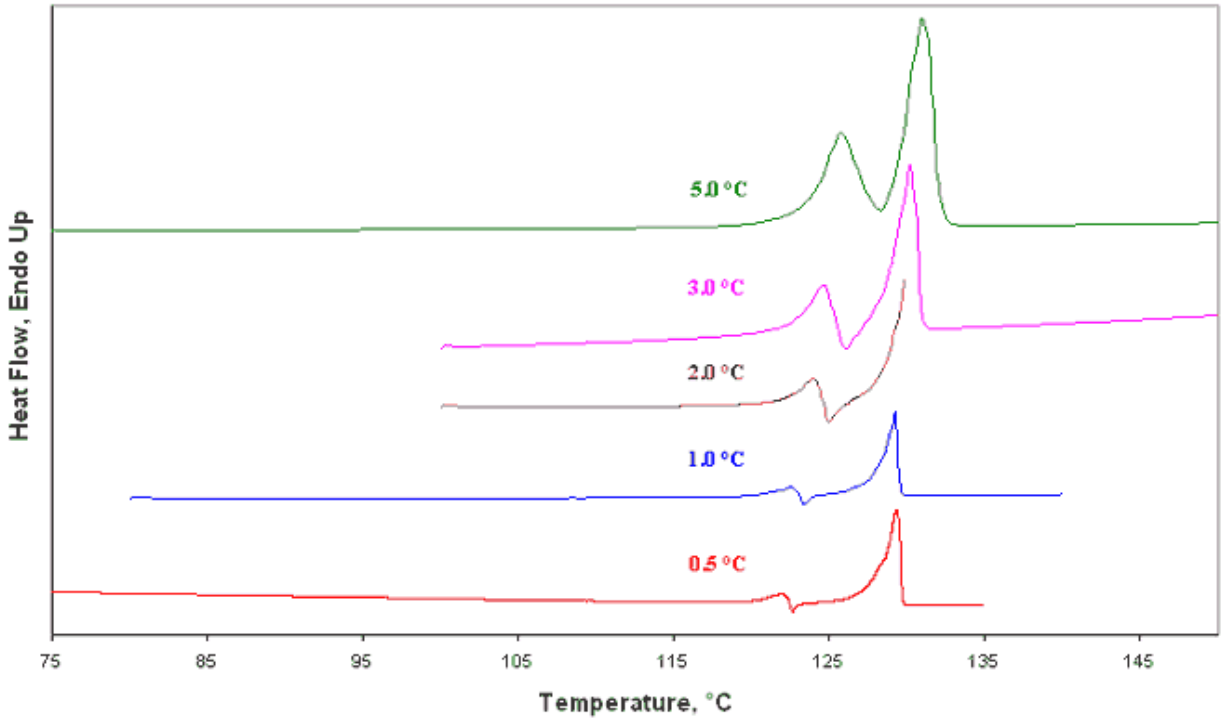

Figure 2. DSC of polymorph A at different heating rates.

Leitz, Heerbrugg, Switzerland) with a tungsten lamp as the light source. The objects were viewed in the magnification range ×200 to ×800.

Scanning Electron Microscopy

The morphology and surface characteristics of the samples were observed by scanning electron microscopy (Cambridge Stereoscan S360, Leo Electron Optics, Thornwood, NY). Samples were mounted on an aluminum scanning electron microscopy (SEM) stub and sputter-coated with gold for 90 seconds at 45 mA. SEM examinations were performed at 5 to 10 kV, 20 pA probe current, and ×100 to ×4000, and at a working distance of 6 to 9 mm.

HPLC Analysis

The amounts of host and guest in CPD + urea cocrystals was assayed by liquid chromatography (HP1100 Series chromatograph, Agilent Technologies, Palo Alto, CA). An isocratic, reverse-phase separation method was developed and validated using external standards following modification in the USP method for CPD. Specific details of the method include Supelco C-18 column (4.6 mm × 15 cm, 5 µ), Mobile Phase composition of 60% dilute acetic acid + 40% acetonitrile at a flow rate of 1.5 mL/min. Sample solutions of 10 µL were injected and detected at 240 nm using a diode array detector. Absence of chromophores in urea limited its detection by the diode array detector in both the UV and visible ranges. The separation, however, was accomplished by the HPLC method, and the interference from urea in the detection of CPD was established to be negligible. The amounts of urea in a mixture were calculated from the CPD levels in the mixture. The accuracy of such calculations was tested at different levels of urea as a part of the HPLC method validation.

Results and Discussion

Polymorphism in CPD

The commercially available form of CPD was obtained by crystallization from ethanol-water mixture and is called form A. It is the most thermodynamically stable form at room temperature and has the lowest dissolution rate. Melt recrystallization of this form results in polymorph B, which is monotropic with form A [24].This form is unstable at all the temperatures and is reported to convert to form A through multiple transformations [16].Polymorph C is obtained by heating form A at 120°C for 4 hours. Taken as a pair, forms A and C are enantiotropically related, form C being the thermodynamically stable form at higher temperatures, while form A is stable at lower temperatures. The transition temperature for this conversion, however, has not been reported to date. DeVilliers and Wurster determined the heats of solution of these forms in dimethylformamide at 25°C [16]. The difference in the heats of solution between these forms was found to be significant (4 kJ/mol) in this study. This was not reflected in the DSC analysis, which failed to show any endotherms corresponding to this heat of transition, even at heating rates as low as 0.5°C/min (**Figure 2**). Conversion of form A to form C as seen during the analysis did not permit calculation of individual melting data for these forms. The thermal behavior of polymorph A was therefore investigated in detail. As can be seen

from **Figure 2**, subjecting form A to DSC analysis at different heating rates revealed some interesting results. The endotherm at 121°C corresponds to the melting of form A, while the one at 129°C corresponds to that of form C. The transition from A to C was found to occur gradually with increase in temperature and was most rapid at temperatures nearing the melting point of A. Apparently, the melting endotherms overlap, making the heat of fusion values for these polymorphs indeterminable. Efforts at resolving these melting endotherms by reducing the heating rates revealed intermediate recrystallization that was hidden at higher heating rates. Thermomicroscopy simulating the heating ramps used in the above DSC analysis revealed that the transition from A to C is rapid around the melting point of A but does not necessarily occur from the melt. Apparent change in the particle morphology was seen upon gradually heating from 100 to 120°C. TGA of polymorph A did not indicate any weight loss around this temperature, excluding the possibility of solvent/water-mediated transition. From the discussion above, it can be stated that the transition from A to C occurs in a solid state with no change in the composition of the solid. It was hoped that the intermediary recrystallization exotherm could be separated as a kinetic event, utilizing the modulations in heating by mDSC. The result of mDSC performed at a heating rate of 1°C/min is shown in **Figure 3**. The thermogram in the temperature range 25 to 80°C was uneventful and hence is not shown in the figure. As can be seen from the reversing (enthalpy related) curve in **Figure 3**, even this method failed to isolate the 2 endotherms. This indicates that a reversible transformation between forms A and C occurs just before form A melts. Calculation of the heat of fusion value of form A, to be utilized in evaluating its crystallinity, is therefore not possible by direct DSC analysis. For the purposes of this study, this value was calculated from the $\Delta H_f$of form C in a manner analogous to the Behme and Brooke study [25].Unlike in the case of carbamazepine, the transition from one polymorph to the other did not occur during the DSC analysis of CPD. For this study, this heat of transition was estimated to be 4 kJ/mol (or 14.45 J/g), the difference in the heats of solution values reported by DeVilliers at 25°C. This estimation was made on the basis that a linear relationship exists between the heat of solution and the heat of fusion for the same polymorph with a fixed chemical structure [26].Such an estimation is further supported by the Hess Law, which states that the energy associated with a transition depends on the final states and is independent of the path. Assuming that this difference is constant over the temperature range of 30 to 120°C, the heat of fusion of form A can be estimated to be 85.77 + 14.45 = 100.22 J/g. This assumption was validated when the heat capacity values (C_p) of polymorphs A and C were found to vary similarly in this temperature range (notice the parallel baselines for various polymorphs in **Figure 4**). The ΔH_fvalues of polymorphs B and C are obtained from the DSC analysis, given that these polymorphs can be produced in pure form and no concurrent phase changes occur during their thermal analysis. The melting

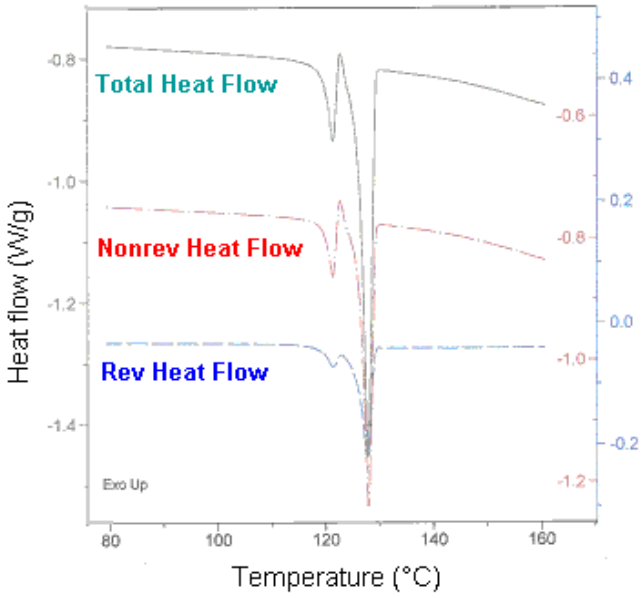

Figure 3. Results of mDSC analysis.

data for polymorphs A, B, and C, following the above discussion, are summarized in **Table 1**.Two other means of characterizing the various polymorphs of CPD were also developed. The first used polarizing optical microscopy. As can be seen in **Figure 5** , the various polymorphs' crystal habits appear to be distinctly different. Polymorph A seems to crystallize in a tabular habit, while the metastable forms B and C appear as blades and plates respectively. In addition, XRPD serves as a very powerful tool in distinguishing these polymorphs. The diffraction patterns of the 3 forms are shown in **Figure 6**. The major diffraction peaks distinguishing the various polymorphs are shown in **Table 1**. In summary, polymorphs A, B, and C are characterized by various analytical techniques, and the results are summarized in **Table 1**. Also, the thermodynamic data useful in evaluating the crystallinity of these polymorphs in the later doping studies is developed (**Table 1**).

RESS of Pure CPD

Pure CPD was recrystallized from supercritical CO_2at 8 combinations of temperature (4) and pressure (2). Increased yields from crystallization were achieved upon increasing both the extraction pressure and the temperature of supercritical CO_2. Recrystallization of polymorph A from supercritical CO_2at different pressure and temperature conditions resulted in the formation of several metastable polymorphs (**Table 2**). Of interest here in view of enhancing the dissolution performance is the formation of polymorph C, which dissolves at least twice as fast as form A [14].While complete polymorph conversion from A to C was seen at certain conditions, the original form remained at other extraction temperatures and pressures (**Table 2**). The polymorphic identity of the

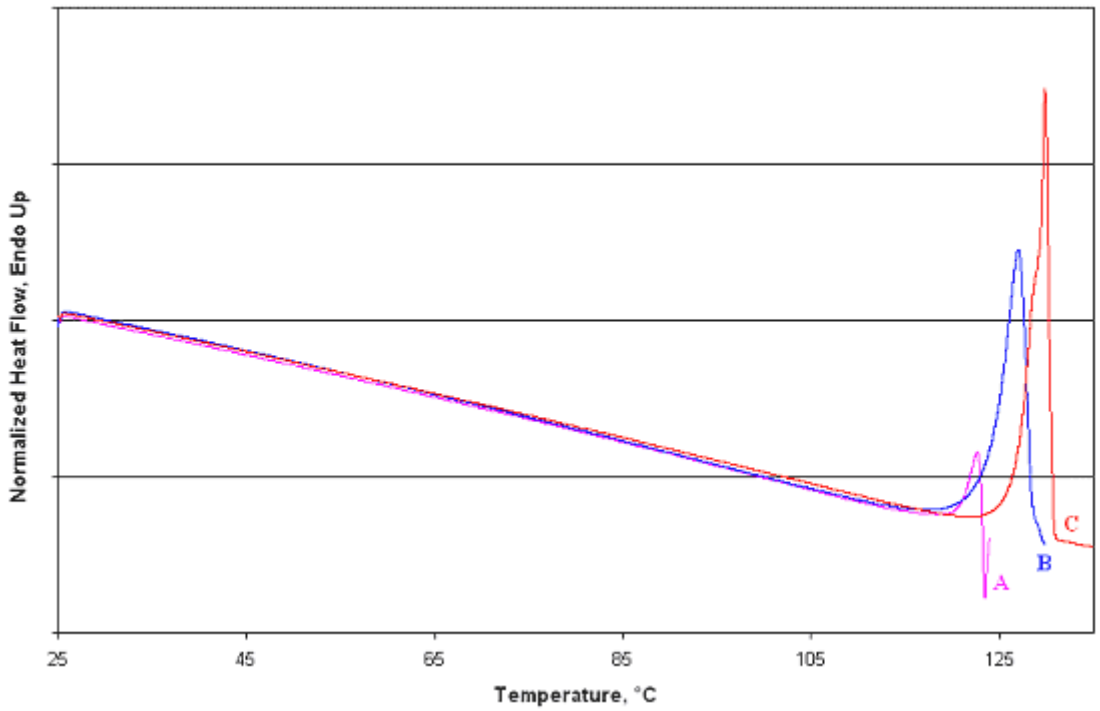

Figure 4. Thermograms of different polymorphs of CPD.

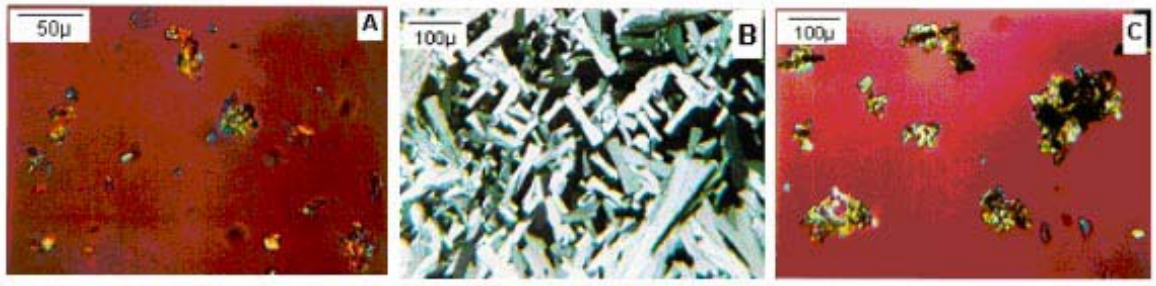

Figure 5. Photomicrographs of polymorphs A, B, and C of CPD.

RESS-recrystallized materials was positively confirmed from their XRPD data (**Figure 7**). On the other hand, the thermal behavior of RESS-recrystallized materials as determined by DSC exhibited inconsistency with the XRPD results in certain cases. The melting temperatures, however, exactly match Burger's polymorphs denoted by the Roman nomenclature (**Table 1**) [13].XRPD data for these polymorphs were not reported in Burger's study, and hence no definitive matches could be made.

The results of RESS recrystallizations of pure CPD indicate the ability of the RESS process to form different polymorphs from the same solvent by mere changes in the temperature and pressure conditions. The polymorphic conversion from form A to form C can be explained based on the individual effects of temperature and pressure on the CPD crystallites during their nucleation and growth. The effect of temperature on this conversion was addressed in detail in the preceding section. This conversion upon recrystallization from SC $CO_2$is consistent with the reported effects of temperature and compression pressure during the tableting of CPD [27].It appears from these studies that these forms differ in the manner of their packing, which is easily influenced by the temperature and pressure during SCF crystallization.

SEM of recrystallized materials indicated a change in the habit and a general reduction in the particle size of the recrystallized materials (**Figure 8**). Agglomeration of the particles arising from bouncing against each other and against the walls of the small 40 ml collection vial can be seen in relation to rather distinct crystals collected in a larger 1L vessel (compare **Figures 8b-8e** with **Figure 8f**). While a tabular habitat can be seen in the commercially available material, all the RESS-recrystallized samples attained the blade shape typical of form C. Consistent with the XRPD results, CPD recrystallized from selective RESS conditions contained both the forms A and C reflected as a mix of tabular and platelike crystals (**Figures 8b, 8c, 8d**). Also, particle size reduc-

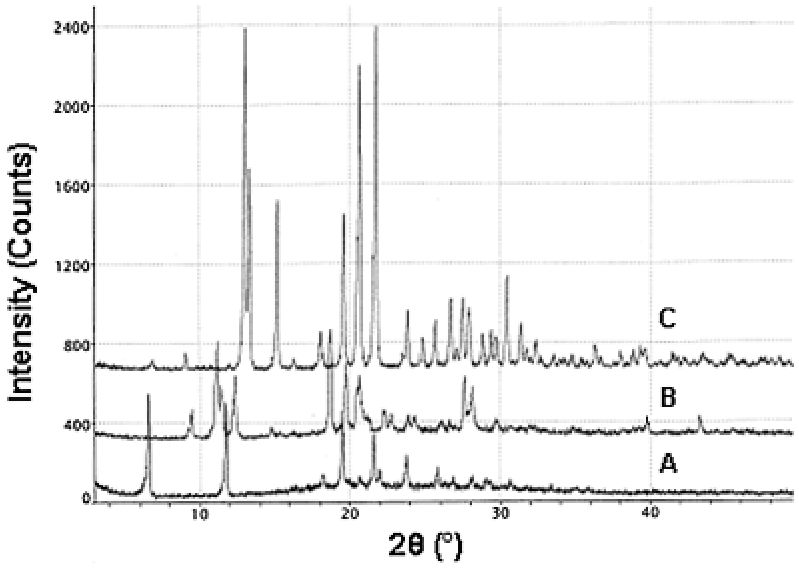

Figure 6. XRPD patterns of polymorphs A, B, and C of CPD.

Table 2. Polymorph Conversion of Chlorpropamide by RESS Recrystallization*

Conditions of Rxn Vessel (T in °C, P in psi)	T_m °C (RSD)	Delta H_f (J/g) (RSD)	Polymorph Identity (XRPD)
46, 4000	112.43 (1.51)	23.67 (8.99)	C
48, 8000	122.05 (1.01)	49.97 (1.31)	C
60, 4000	111.58 (0.47)	32.99 (5.70)	A + C
61, 8000	117.50 (0.43)	54.14 (1.82)	A + C
75, 4000	126.58 (0.23)	68.63 (2.06)	A + C
75, 8000	127.08 (0.30)	70.72 (3.66)	C
101, 4000	124.56 (0.95)	60.43 (1.18)	A + C
100, 8000	125.58 (0.41)	62.62 (1.08)	C

*RESS indicates rapid expansion of supercritical solution; Rxn, reaction; T, temperature; P, pressure; RSD, relative standard deviation; XRPD, x-ray powder diffractometry.

tion was significant at the 75°C condition, perhaps because of higher supersaturation attained at this temperature than at the 60°C condition. As can be seen from **Figures 8a to 8f**, submicron- to few-micron-sized particles were produced by RESS recrystallization.

RESS of CPD + Urea

The presence of urea in the crystallizing medium of CPD reduced the overall yields. The solubility of CPD appears to be significantly higher than urea in SC CO_2at the various conditions studied. An apparent reduction in the overall yields can therefore be expected in the presence of a less soluble component like urea. The binary phase behavior of CPD + urea mixtures was studied by Ford and Rubienstein [28].who reported that a mixture containing 89% CPD + 11% urea forms a eutectic that melts at 89°C. Compositions containing >90% CPD were reported to form solid solutions. This region is of particular interest in the context of crystal doping. Cocrystallization of CPD in the presence of urea resulted in the formation of eutectic mixtures and solid solutions depending on the composition of the mixtures formed (**Tables 3** and **4**). An agreement between the thermal behavior of the cocrystals and their compositions can be seen from **Tables 3** and **4**.

Formation of the solid solutions of urea in CPD resulted in the crystal disruption of the host and eventually in amorphous conversion at urea levels higher than 40% wt/wt (**Figure 9**). Peak broadening and peak shifts in the x-ray diffraction patterns were seen in all the doped crystals (**Table 5**). Two mechanisms are proposed that caused this consistent broadening and shifts in the XRPD peaks, as illustrated in **Figure 10**. First, as shown in mechanism 1, urea may have been adsorbed onto selective faces of the crystals that apparently changed the way CPD packs. This led to altered symmetry and increased mosaic spread, as evidenced by the manner in which different planes reflect x-rays. Apparently, peak broadening and a shift in the XRPD peaks is seen. Another fact that further validates this mechanism is the preferential crystallization of polymorph C in the presence of urea. By adsorbing onto selective faces, urea may have mediated crystallization of polymorph C while

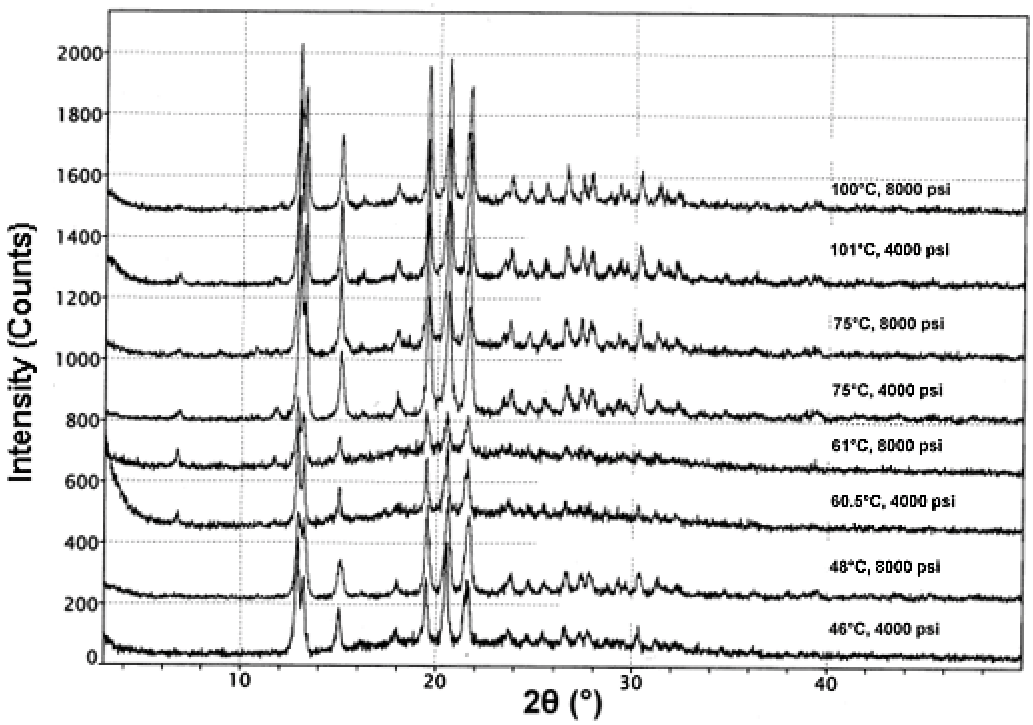

Figure 7. XRPD patterns of RESS-produced CPD.

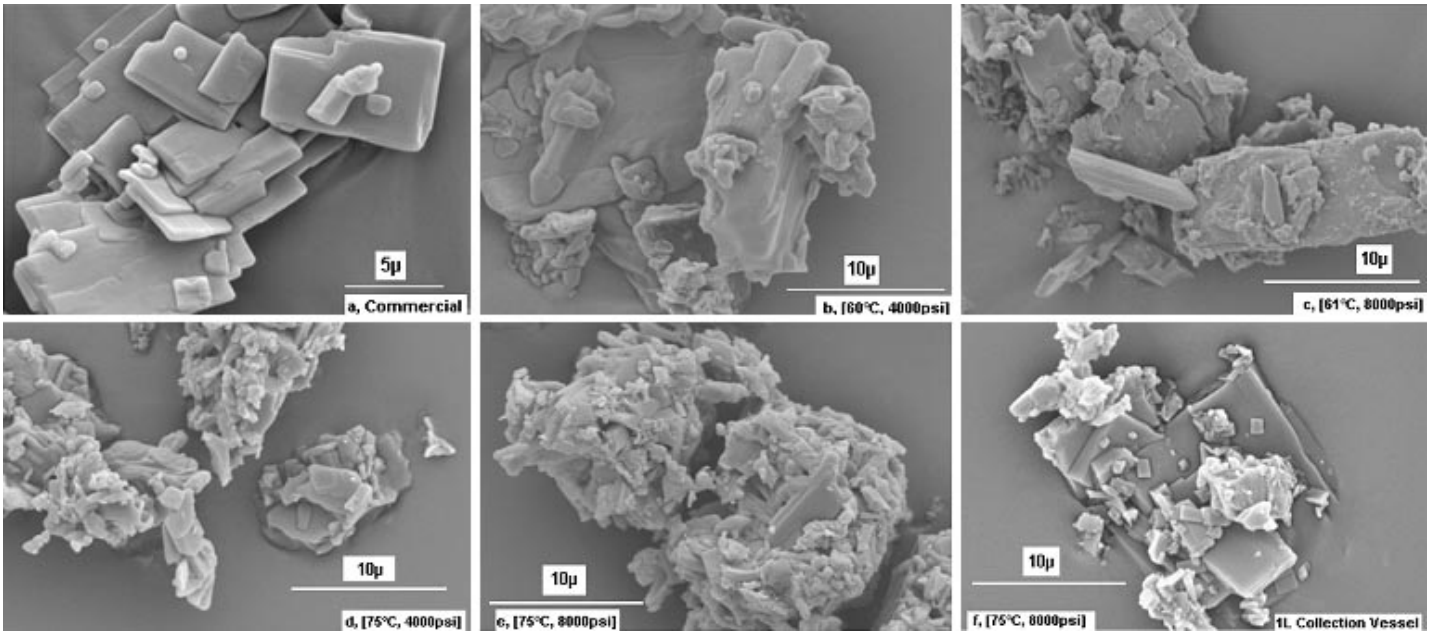

Figure 8. SEM images of pure CPD (a) and RESS-recrystallized drug from SC CO_2.

stunting the growth of A. The second mechanism involves the inclusion of urea into the lattice of CPD, increasing the volume of the crystal lattice, and thereby increasing the d-spacings. Increased volume as a result of the distortion induced by a foreign molecule also results in the shift of XRPD peaks. Interestingly, this is reflected in the majority of the peaks shifting toward the lower 2θs. A combination of these 2 mechanisms is also possible where the levels of impurity are high, culminating in the eventual loss of symmetry and subsequent amorphous conversion. Although single-crystal data of the doped crystals will provide more insight into such mechanisms, single crystals are difficult to grow to tangible sizes using SCF recrystallization. On the other hand, the XRPD data

Table 3. Selectivity of Extraction as a Function of T/P of Supercritical Carbon dioxide*

Extraction Conditions (T in °C, P in psi)	CO_2 Density (g/cc)	Average CPD (%)	RSD (n = 3)	Urea (%)
48, 4000	0.8631	—	—	—
48, 8000	0.9852	85.87	1.07	14.13
60, 4000	0.8109	93.09	3.43	6.91
61, 8000	0.9509	93.55	3.12	6.45
75, 4000	0.7431	98.38	0.82	1.62
77, 8000	0.9055	85.61	5.48	14.39
100, 4000	0.6287	60.57	4.84	39.43
103, 8000	0.8355	42.08	0.95	57.92

*T indicates temperature; P, pressure; CPD, chlorpropamide; RSD, relative standard deviation.

Table 4. Results of Doping Chlorpropamide With Urea*

Conditions of Rxn Vessel (T in °C, P in psi)	Tm °C (RSD)	ΔH_f (RSD) (J/g), n = 3	Polymorph Identity
48, 4000	123.42 (0.23)	47.40 (7.03)	C
48, 8000†	No drug peak	—	C
60, 4000†	118.29 (0.66)	44.96 (5.17)	A + C
61, 8000†	121.08 (1.33)	54.80 (5.45)	C
75, 4000	121.57 (0.23)	40.01 (4.30)	C
77, 8000	119.58 (0.97)	26.39 (11.34)	C
100, 4000	No drug peak	—	C/amorphous
103, 8000	No drug peak	—	Amorphous

* Rxn indicates reaction; T, temperature; P, pressure; RSD, relative standard deviation
† Eutectic mixture formed.

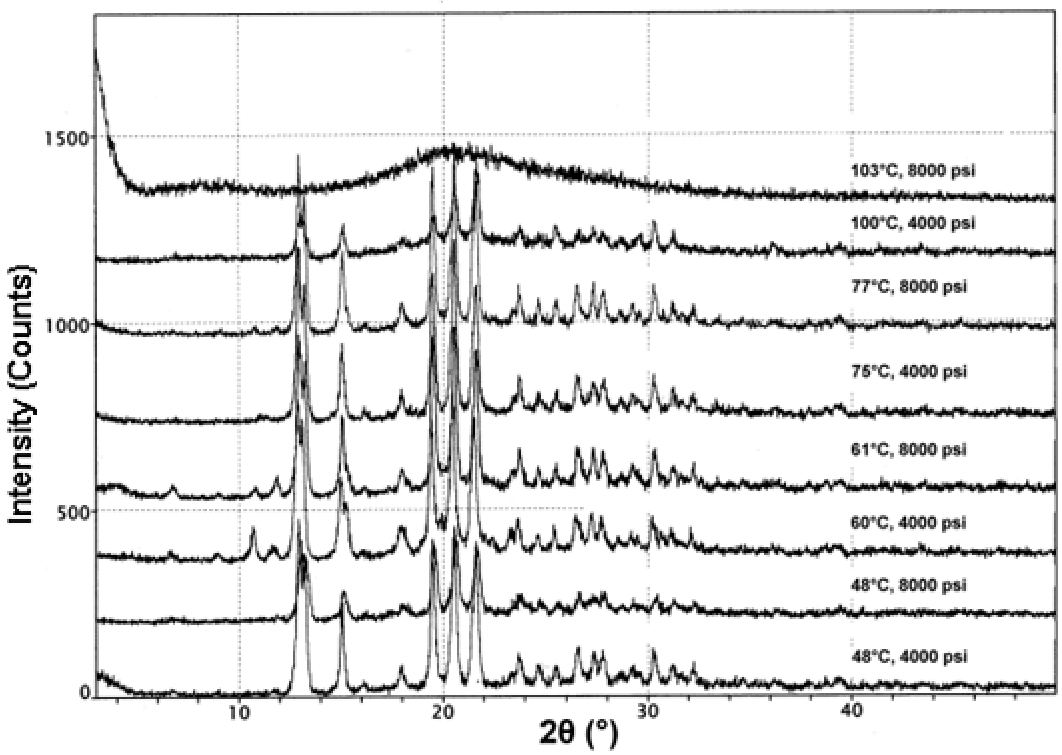

Figure 9. XRPD patterns of RESS-produced cocrystals of CPD + urea.

Table 5. Peak Shifts and Peak Broadening in Doped Chlorpropamide Crystals*

Percent Urea	FWHM Values									
	2θ=13.04	2θ=15.18	2θ=18.04	2θ=20.68	2θ=21.76	2θ=26.66	2θ=29.7	2θ=30.42	2θ=31.34	2θ=32.36
0	0.18	0.15	0.19	0.18	0.17	0.18	0.18	0.15	0.18	0.17
0.00	**0.43**	*0.19*	*0.21*	**0.25**	**0.27**	0.22	**0.48**	**0.21**	**0.64**	**0.3**
1.62	**0.51**	*0.2*	*0.16*	*0.25*	*0.27*	*0.23*	**0.4**	*0.22*	-	-
6.45	**0.38**	**0.25**	**0.29**	*0.22*	*0.25*	**0.24**	**0.35**	-	-	**0.38**
6.91	**0.41**	**0.46**	**0.33**	*0.21*	*0.25*	**0.31**	-	-	-	-
14.13	**0.48**	**0.27**	*0.28*	**0.29**	**0.29**	-	**0.34**	**0.29**	**0.48**	*0.11*
14.39	**0.41**	*0.25*	**0.32**	-	*0.24*	*0.23*		**0.33**	**0.37**	**0.41**
39.43	**0.41**	*0.21*	-	*0.27*	*0.26*	*0.13*	*0.2*	*0.24*	**0.3**	-
57.92	AMORPHOUS CONVERSION									

* FWHM indicates full width at half maximum; Bold font: Broadened Peaks; Italic font: Shifted Peaks

generated in this study can be utilized in deducing the lattice parameters and other crystallographic data by iterative computer simulations. Published single-crystal data are available for only form A [29], and such studies could not be performed for polymorph C, which was frequently formed in these studies. The evidence of crystal disruption was also confirmed by the lowering of the melting points and the heat of fusion values of the doped crystals compared to pure crystal of the same polymorph (**Table 4**). Melting point reductions up to 9°C were seen upon doping with urea. Also, significant reductions in the ΔH_fvalues of CPD up to 50% were seen as a result of doping with urea. By imparting a strain in the lattices of CPD crystals that was observed in XRPD results, urea may have reduced the symmetry in the original crystals. This explains the reductions in the heat of fusion values seen in doped CPD crystals. Such reductions manifest themselves in significant increases in the initial dissolution rates owing to the ease with which the solvent can destroy the crystal structure for subsequent dissolution. Following the log-linear relationship observed between these entities by Yoshihashi et al [26].projected enhancement in the initial dissolution rates can be expected to be significant.SEM of the doped crystals indicated surface precipitation of urea onto CPD crystals (**Figure 11**). The differential rates of precipitation of CPD and urea still prevailed in spite of the structural similarity between them and the rapid expansion conditions. Knowledge of the solubility behavior of individual components in the SCF can be of potential value in this context. Also, the particles appeared severely agglomerated because of the use of a small collection vial. Given that the interest here was in the crystalline morphology of the RESS-produced crystals of CPD, no exhaustive attempts were made to restore the microcrystals formed by SC $CO_2$from agglomeration. To prove the concept that agglomeration arises from the bouncing of particles released at high velocities into the collection vessel (40 mL), a larger collection vessel was used (1 L). Because of the altered dynamics of jet expansion in this case, agglomeration was significantly reduced (compare **Figure 11f** with **Figures 11b-11e**). The SEM images shown in **Figure 11f** indicate that the particle size of the primary RESS-produced particles is in the range of 1 to 2 μ, while that of the starting material was around 10 μ. A particle size reduction of up to an order of magnitude was therefore produced upon RESS processing.

The efficiency of the RESS process in doping was evaluated by direct comparison to the doped crystals produced from liquid organic solvents. Polymorphic conversion was not seen in CPD recrystallized from ethanol, ethyl acetate, or hexane. XRPD results of these materials indicated that polymorph A was formed in all the solvent systems, irrespective of their polarities.

Although minor reductions in the melting temperatures and the heat of fusion values of CPD were seen upon doping with urea (**Tables 6**, **7**, and **8**), no significant disruption in the crystallinity was evident from the XRPD results. A possible cause may be that only limited amounts of urea actually incorporated into the lattice of CPD. On the other hand, the fast nucleation and growth from a supercritical solution may have locked rather high levels of urea into the crystal lattice of the host, causing large reductions in the crystallinity. The ability to adjust the level of impurity in this context provides the control over the levels of crystallinity of CPD. This feature of RESS-based crystal doping coupled with the polymorph conversion and particle size reduction capabilities may all be advantageously utilized toward enhancing the dissolution rates of poorly soluble drugs.

CONCLUSION Toward the objective of enhancing the dissolution characteristics of poorly soluble drugs, amorphization of APIs is increasingly popular in today's developmental research. A more subtle crystal modification approach, if applied early in the development process, may ease subsequent development work. It is with this objective that the polymorph conversion and crystal disruption of a model API, CPD, were accomplished in this study. The results reflect the potential for RESS-aided crystal doping in not only controlling the crystallinity levels in APIs but also tailoring the polymorphism and

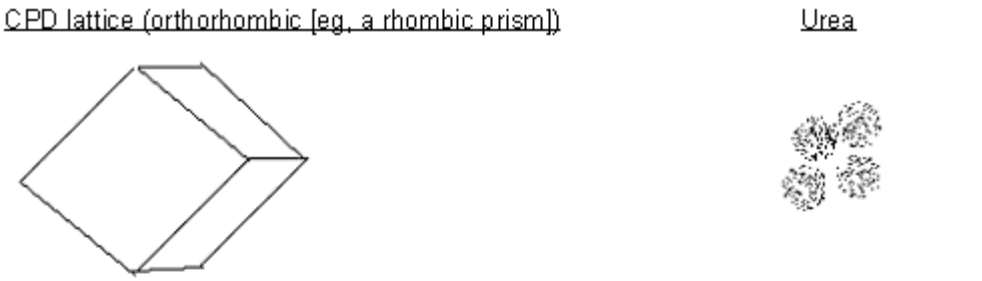

Mechanism 1: Selective adsorption of different faces

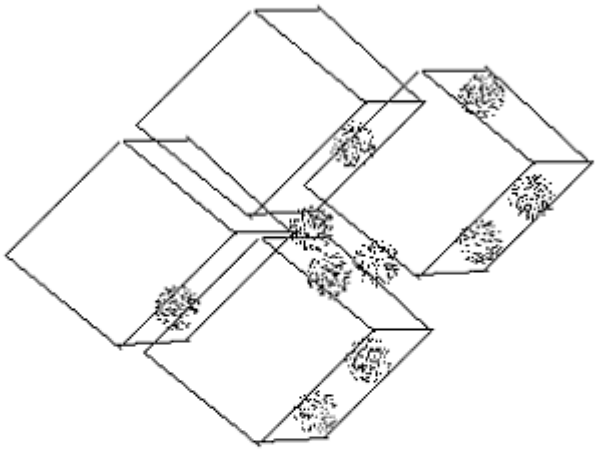

Mechanism 2: Inclusion → volumetric expansion→ loss of symmetry→ amorphous conversion

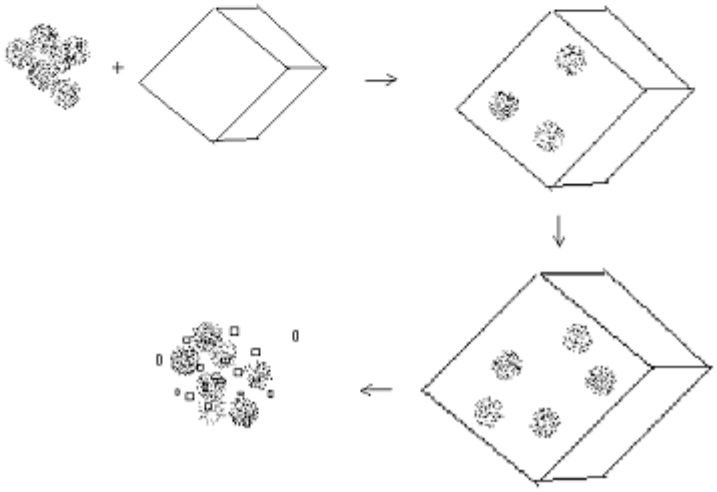

Figure 10. Illustration of the proposed mechanisms of crystal disruption.

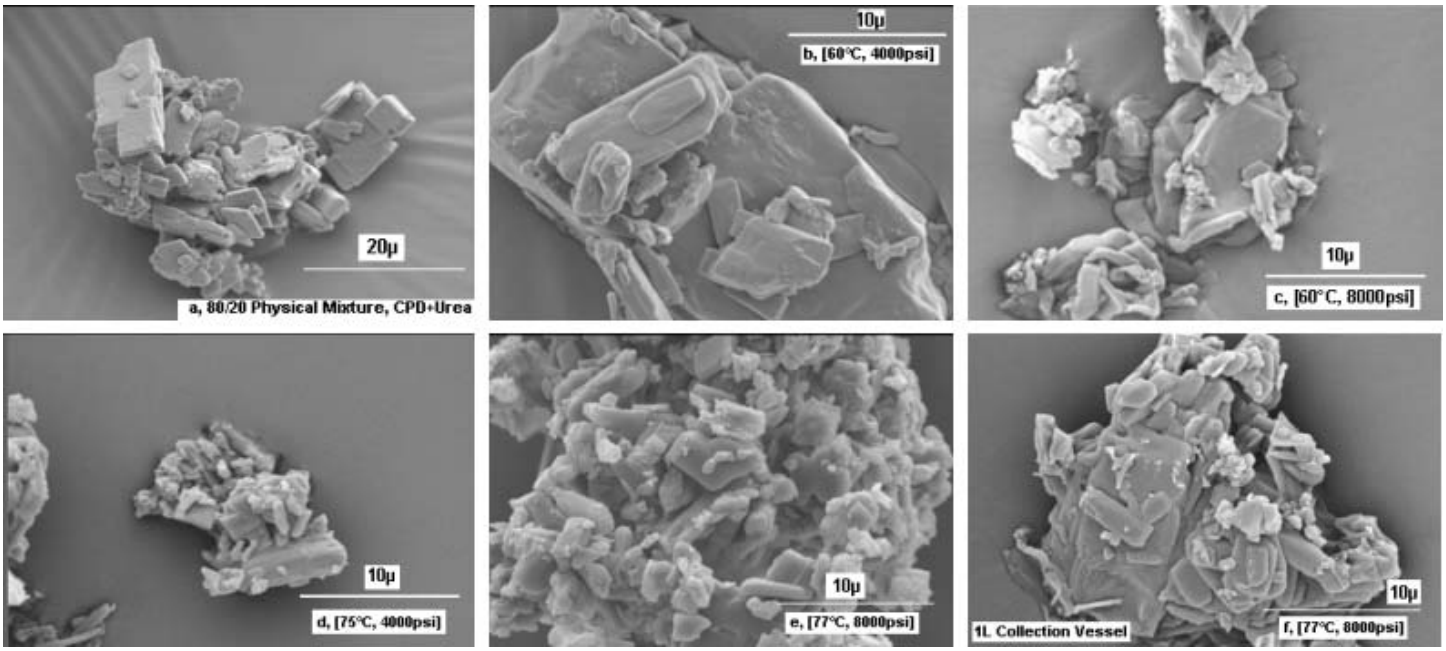

Figure 11. SEM images of CPD + urea physical mixture (a) and RESS-produced cocrystals.

Table 6. Thermal Analysis of CPD + Urea Mixtures Recrystallized From EtOH*

Sample	Endotherm 1 (°C)	$\Delta H_f 1$ (J/g)	Endotherm 2 (°C)	$\Delta H_f 2$ (J/g)
80% CPD + 20% urea	98.63 (0.33)	54.81 (2.80)	122.67 (0.92)	3.88 (2.36)
90% CPD + 10% urea	96.07 (0.51)	56.80 (19.92)	—	—
99.5% CPD + 0.5% urea	117.20 (0.85)	5.90 (32.99)	126.33 (0.54)	54.34 (4.19)
99.9% CPD + 0.1% urea	112.95 (0.62)	60.73 (12.95)	—	—

*CPD indicated chlorpropamide.
† Values within parenthesis are respective relative standard deviations.

Table 7. Thermal Analysis of Chlorpropamide + Urea Mixtures Recrystallized From EtAc*

Sample	Endotherm 1 (°C)	$\Delta H_f 1$ (J/g	Endotherm 2 (°C)	$\Delta H_f 2$ (J/g)
Pure CPD	119.97 (0.65)	8.41 (4.63)	128.95 (0.41)	76.97 (2.20)
80% CPD + 20% urea	95.83 (0.40)	68.11 (19.14)	125.42 (0.23)	3.97 (25.03)
90% CPD + 10% urea	106.11 (0.24)	87.55 (2.30)	—	—
99% CPD + 1% urea	116.38 (0.34)	21.19 (58.34)	124.43 (0.50)	53.35 (9.68)
99.5% CPD + 0.5% urea	117.38 (0.48)	22.13 (73.28)	126.63 (0.52)	70.39 (2.43)
99.9% CPD + 0.1% urea	118.56 (0.13)	17.59 (8.21)	127.86 (0.12)	72.44 (1.20)

*CPD indicates chlorpropamide.
† Values within parenthesis are respective relative standard deviations.

Table 8. Thermal Analysis of Chlorpropamide + Urea Mixtures Recrystallized From Hexane*

Sample	Endotherm 1 (°C)	ΔH_f 1 (J/g)	Endotherm 2 (°C)	ΔH_f 2 (J/g)	Endotherm 3 (°C)	ΔH_f 3 (J/g)
Pure CPD	122.83 (0.42)	16.25 (11.72)	129.58 (0.11)	82.596 (1.83)	—	—
80% CPD + 20% urea	99.00 (0.25)	77.48 (3.52)	115.50 (0.75)	9.90 (8.69)	—	—
99% CPD + 1% urea	100.92 (0.14)	7.92 (100)	115.33 (0.25)	31.10 (8.36)	120.92 (0.43)	32.57 (5.31)
99.5% CPD + 0.5% urea	121.08 (0.66)	9.77 (20.6)	129.25 (0.51)	75.95 (3.62)	—	—
99.9% CPD + 0.1% urea	118.67 (0.49)	9.81 (12.13)	127.42 (0.41)	66.95 (2.22)	—	—

*CPD indicates chlorpropamide.

† Values within parenthesis are respective relative standard deviations.

particle morphology. This body of work further serves as a proof of concept for the application of RESS-aided crystal doping to alter the functionality of APIs in a continuous unit operation. Such studies can serve as a basis for the use of other rapid crystallization processes in the chemical synthesis of materials with desired attributes.

ACKNOWLEDGEMENTS

CV wishes to thank Dr David Pope, Dr Isaac Ghebre-Sellassie and Dr KS Murthy for their valuable suggestions and support. Thanks are also due to Dr Hayden Thomas for help with the SEM experiments.

REFERENCES

1. Cram DJ. The design of molecular hosts, guests and their complexes. Science. 1988;240:760-767.

2. Klarner FG, Panitzky J, Blaser D, Boese R. Synthesis and supramolecular structures of molecular chips. Tetrahedron. 2001;57:3673-3687.

3. Weissbuch I, Leiserowitz L, Lahav M. Tailor-made additives and impurities. In: Mersmann A, ed. Crystallization Technology Handbook. 2nd ed. New York, NY: Marcel Dekker; 2001:563-616.

4. Williams-Seton L, Davey RJ, Lieberman HF, Pritchard RG. Disorder and twinning in molecular crystals: impurity-induced effects in adipic acid. J Pharm Sci. 2000;89(3):346-354.

5. Addadi L. Resolution of conglomerates with the assistance of tailor-made impurities: generality and mechanistic aspects of the "Rule of reversal□—a new method for assignment of absolute configuration. J Am Chem Soc. 1982;104:4610-4617.

6. Jane Li Z, Grant DJW. Effects of excess enantiomer on the crystal properties of a racemic compound: ephedrinium 2-naphthalenesulfonate crystals. Int J Pharm. 1996;137:21-31.

7. Davey RJ, Blagden N, Potts GD, Docherty R. Polymorphism in molecular crystals: stabilization of a metastable form by conformational mimicry. J Am Chem Soc. 1997;119(7):1767-1772.

8. Gu CH, Chatterjee K, Young V, Grant DJW. Stabilization of a metastable polymorph of sulfamerazine by structurally-related additives. AAPS PharmSci. 2001;3(3).

9. Lemieux RP, Dinescu L. Compounds and methods for doping liquid crystal hosts. US Patent 5 989 451. Issued 11-23-1999.

10. Chow AHL, Hsia CK, Gordon JD, Young JWM, Vargha-Butler EI. Assessment of wettability and its relationship to the intrinsic dissolution rate of doped phenytoin crystals. Int J Pharm. 1995;126:21-28.

11. Prasad KVR, Ristic RI, Sheen DB, Sherwood JN. Crystallization of paracetamol from solution in the presence and absence of impurity. Int J Pharm. 2001;215:29-44.

12. Weissbuch I, Addadi L, Lahav M, Leiserowitz L. Molecular recognition at crystal interfaces. Science. 1991;253:637-645.

13. Burger A. Zur Polymorphie oraler Antidiabetika. Sci Pharm. 1975;43:152-161.

14. Aal-Saieq SS, Riley GS. Polymorphism in sulfonylurea hypoglycemic agents, II: chlorpropamide. Pharm Acta Helv. 1982;57(1):8-11.

15. Simmons DL, Ranz RJ, Gyanchandani D. Polymorphism in pharmaceuticals, III: Chlorpropamide. Can J Pharm Sci. 1973;8(4):125-127.

16. De Villiers MM, Wurster DE. Isothermal interconversion of chlorpropamide polymorphs kinetically quantified by XRPD, diffuse reflectance FTIR and isoperibol solution calorimetry. Acta Pharm. 1999;49:79-88.

17. Mohamed RS, Halverson DS, Debenedetti PG, Prud'homme RK. Solids formation after the expansion of supercritical mixtures. In: Johnston KP, Penninger JML, eds. Supercritical Fluid Science and Technology. ACS Symposium Series—406. Washington, DC: American Chemical Society; 1989:355-378.

18. Debenedetti PG, Tom JW, Kwauk X, Yeo SD. Rapid expansion of supercritical solutions (RESS): fundamentals and applications. Fluid Phase Equil. 1993;82:311-321.

19. Turk M. Formation of small organic particles by RESS: experimental and theoretical investigations. J Supercrit Fluids. 1999;15:79-89.

20. Burt HM, Mitchell AG. Crystal defects and dissolution. Int J Pharm. 1981;9:137-152.

21. Hyatt JA. Liquid and supercritical carbon dioxide as organic solvents. J Org Chem. 1984;49:5097-5101.

22. Dandge DK, Heller JP, Wilson KV. Structure solubility correlations: organic compounds and dense carbon dioxide binary systems. Indus Eng Chem Prod Res Dev. 1985;24:162-166.

23. Dobbs JM, Wong JM, Lahiere RJ, Johnston KP. Modification of supercritical fluid phase behavior using polar cosolvents. Indus Eng Chem Res. 1987;26:56-65.

24. Yu L. Inferring thermodynamic stability relationship of polymorphs from melting data. J Pharm Sci. 1995;84(8):966-974.

25. Behme RJ, Brooke D. Heat of fusion measurement of a low melting polymorph of carbamazepine that undergoes multiple phase changes during DSC. J Pharm Sci. 1991;80(10):986-990.

26. Yoshihashi Y, Kitano H, Yonemochi E, Tereda K. Quantitative correlation between initial dissolution rate and heat of fusion of drug substances. Int J Pharm. 2000;204:1-6.

27. Otsuka M, Matsumoto T, Higuchi S, Otsuka K, Kaneniwa N. Effects of compression temperature on the consolidation mechanism of chlorpropamide polymorphs. J Pharm Sci. 1995;84(5):614-618.

28. Ford JL, Rubinstein MH. Phase equilibria and stability characteristics of chlorpropamide-urea solid dispersions. J Pharm Pharmacol. 1977;29:209-211.

29. Koo CH, Cho SI, Yeon YH. The crystal and molecular structure of chlorpropamide. Arch Pharm Res. 1980;3(1):37-49.